

African Journal of Herpetology



ISSN: (Print) (Online) Journal homepage: www.tandfonline.com/journals/ther20

Population genetics and phylogeography of *Trachylepis sulcata* (Peters, 1867) and *T. ansorgii* (Boulenger, 1907) in south-western Africa

Brett O Butler, Luis MP Ceríaco, Todd R Jackman & Aaron M Bauer

To cite this article: Brett O Butler, Luis MP Ceríaco, Todd R Jackman & Aaron M Bauer (18 Jul 2024): Population genetics and phylogeography of *Trachylepis sulcata* (Peters, 1867) and *T. ansorgii* (Boulenger, 1907) in south-western Africa, African Journal of Herpetology, DOI: 10.1080/21564574.2024.2357758

To link to this article: https://doi.org/10.1080/21564574.2024.2357758

+	View supplementary material ☑ discontinuous
	Published online: 18 Jul 2024.
	Submit your article to this journal 🗗
a a	View related articles 🗷
CrossMark	View Crossmark data 🗗



Population genetics and phylogeography of *Trachylepis* sulcata (Peters, 1867) and *T. ansorgii* (Boulenger, 1907) in south-western Africa

Brett O Butler [©] ^{a,b}, Luis MP Ceríaco [©] ^{c,d,e}, Todd R Jackman^f and Aaron M Bauer [©] ^f

^aMuseo de Zoología "Alfonso L Herrera", Facultad de Ciencias, Universidad Nacional Autónoma de México, Coyoacán, Mexico City, Mexico; ^bPosgrado en Ciencias Biológicas, Universidad Nacional Autónoma de México, Coyoacán, Mexico City, Mexico; ^cCIBIO, Centro de Investigação em Biodiversidade e Recursos Genéticos, InBIO Laboratório Associado, Universidade do Porto, Vairão, Portugal; ^dBIOPOLIS Program in Genomics, Biodiversity and Land Planning, CIBIO, Vairão, Portugal; ^eDepartamento de Vertebrados, Museu Nacional, Universidade Federal do Rio de Janeiro, Quinta da Boavista, São Cristóvão, Rio de Janeiro, Brasil; ^fDepartment of Biology and Center for Biodiversity and Ecosystem Stewardship, Villanova University, Villanova, Pennsylvania, U.S.A.

ABSTRACT

Ansorge's Rock Skink Trachylepis ansorgii (Boulenger, 1907) is an Angolan taxon, the taxonomic distinctiveness and geographic distribution of which are poorly understood. It is closely related to the widespread Western Rock Skink T. sulcata (Peters, 1867) from Namibia and South Africa, but heretofore a lack of samples has prevented a comprehensive assessment of T. ansorgii in a molecular phylogenetic context. We combine new genetic sampling from south-western Angola, including topotypical material of *T. ansorgii*, with published sequences from South Africa and Namibia to identify population structure, phylogenetic relationships, and divergence dates within this species complex. A multi-locus dataset of three nuclear and two mitochondrial loci recovered significant population structuring with a centre of diversity in south-western Angola and northern Namibia. Mitochondrial data recovered seven clades representing distinct geographic populations, while the nuclear data supported either two or three deeper groupings. Mito-nuclear discordance was observed with respect to the geographic boundary between T. ansoraii and T. sulcata. The nuclear data support a break along the western Kunene River (the political boundary between Angola and Namibia), while the mitochondrial data support this break ~250 km to the north in south-western Angola. A timecalibrated BEAST phylogeny found the deepest species-level divergence to have occurred in the late Miocene/early Pliocene (~6 mya), potentially related to the formation of the Kunene River. Our results support the recognition of both taxa at the species level, and add further evidence that south-western Angola is a centre of reptile diversity.

RESUMO

ARTICLE HISTORY

Received 19 December 2023 Accepted 16 May 2024

ASSOCIATE EDITOR HM Faroog

KEYWORDS

Angola; biodiversity; herpetology; Mabuyinae; multi-locus; western rock skink

CONTACT Brett O Butler redgcko7@gmail.com © 2024 Herpetological Association of Africa Supplemental data for this article can be accessed here: https://doi.org/10.1080/21564574.2024.2357758

African Journal of Herpetology is co-published by NISC Pty (Ltd) and Informa Limited (trading as Taylor & Francis Group)

A lagartixa-das-rochas-de-Ansorge, Trachylepis ansorgii (Boulenger, 1907) é um táxon angolano do qual pouco se sabe relativamente à sua identidade taxonómica e distribuição geográfica. Sendo parente próxima da consideravelmente amplamente distribuída lagartixa-das-rochas-ocidental, T. sulcata (Peters, 1867), da Namíbia e África do Sul, a falta de amostras têm até ao momento impossibilitado uma revisão molecular completa da *T. ansorgii*. Juntando novas amostras genéticas do sudoeste de Angola, onde se incluí material topotipico de T. ansorgii, com sequências já publicadas originárias da África do Sul e da Namíbia, podemos identificar a estrutura populacional, relações filogenéticas, e tempos de divergência no seio deste complexo de espécies. Um conjunto de dados de três genes nucleares e dois genes estruturação revelou uma mitocondriais. populacional significativa, com um centro de diversidade no sudoeste de Angola e norte da Namíbia. Os dados mitocondriais revelaram sete clados, cada um representando populações geográficas distintas, enquanto os dados nucleares suportam entre dois ou três grupos. Os dados mitocondriais e nucleares apresentam resultados discordantes, especialmente em relação à fronteira geográfica entre T. ansorgii e T. sulcata. Os dados nucleares apontam uma separação clara no rio Cunene, na fronteira entre Angola e a Namíbia, enquanto os dados mitocondriais sugerem que esta separação é cerca de 250 km a norte, no sudoeste de Angola. Uma árvore BEAST calibrada temporalmente encontrou que a divergência a nível de espécie mais profunda terá ocorrido Miocénico/início do Pliocénica (~6 no final do potencialmente relacionada com a formação do rio Cunene. Os nossos resultados suportam o reconhecimento dos dois taxa como espécies válidas, e trazem novas evidências de que o sudoeste de Angola é um centro de diversidade de répteis.

Introduction

The mabuyine skink genus *Trachylepis* is taxonomically and ecologically diverse, with 97 species currently recognised, mostly in mainland Africa and Madagascar (Uetz et al. 2023; Ceríaco et al. 2024). The position of the genus within Mabuyinae has been addressed (Mausfeld et al. 2002; Karin et al. 2016; Metallinou et al. 2016), while a species level phylogeny including most of the recognised *Trachylepis* taxa was presented by Weinell et al. (2019). Although several problematic species groups have been resolved within this scincid genus (Portik and Bauer 2012; Ceríaco et al. 2016a; Weinell and Bauer 2018), taxonomic uncertainties still remain in some groups. This includes several species complexes occurring in Angola, which until recently was largely inaccessible to researchers due to its four decade-long civil war. A comprehensive review of *Trachylepis* skinks in Angola was recently published by Ceríaco et al. (2024), which described seven new species for the country and elevated three subspecies to full species status, one of which is the focus of this study.

The Western Rock Skink *Trachylepis sulcata* (Peters, 1867) is a viviparous skink widely distributed across south-western Africa, from the western half of South Africa through Namibia and into south-western Angola (Mertens 1955; Branch 1998; Portik et al. 2010; Marques et al. 2018). The taxon was originally described from "Neu-Barmen" [= Gross

Barmen], Otjozondjupa Region, central Namibia (Peters 1862), and two other non-nominotypic forms have been historically recognised. Trachylepis sulcata nigra (Werner, 1915) was described from Lüderitz Bay in southern coastal Namibia based on its distinct melanistic colouration; however, molecular data presented by Portik et al. (2010) revealed that the melanism in this population represents a localised adaptation to the cooler coastal region with high fog cover, a pattern also seen in other African lizards (Daniels et al. 2004; Engelbrecht et al. 2011; Ceríaco et al. 2016a), and the subspecies was consequently synonymised with the nominotypical form. The other form associated with T. sulcata is Ansorge's Rock Skink Trachylepis ansorgii (Boulenger, 1907), a poorly known taxon described from Huíla Province in south-western Angola (Boulenger 1907).

A phylogeographic study of *T. sulcata* by Portik et al. (2011) included extensive sampling from South Africa and Namibia, but tissue samples from Angolan populations were unavailable at the time, preventing any explicit assessment of T. ansorgii. Nevertheless, three distinct groupings were identified within T. sulcata, with the northern Namibian population being the most genetically diverse. The authors hypothesised a Pliocene refugium in this region, with a mid-Pleistocene expansion southward into South Africa (Portik et al. 2011). A phylogeographic break was observed between the southern and central genetic groupings at the Knersvlakte region in the north-western Western Cape province of South Africa (Portik et al. 2011).

The original description of Mabuia Ansorgii (currently Trachylepis ansorgii), based on a single specimen from "Caconda" on the Huíla Plateau, south-western Angola, provided a brief morphological description based on squamation, colouration, and basic measurements (Boulenger 1907). Its taxonomic status, affinities, and distinguishing diagnostic characters have since been debated, with different authors presenting conflicting views (e.g., Boulenger 1907; Monard 1937; Laurent 1964; Mertens 1971; Haacke 1972; Bauer et al. 1993; Branch 1998; Marques et al. 2018; Branch et al. 2019). Mertens (1971) followed Monard (1937) in considering ansorgii as a subspecies (T. sulcata ansorgii) and raised the possibility of the taxon's distribution extending into northern Namibia, with what he considered typical ansorgii specimens from north-western Namibia ("Marienfluß, Kaokkoveld"), while some other Namibian specimens from "Otjitambi" were considered intergrades between ansorgii and sulcata. Haacke (1972) also referred to some specimens on the Namibian side of the Kunene River as T. s. ansorgii. Bauer et al. (1993) noted that while some individuals to the west of the escarpment in north-western Namibia showed the characteristic pinkish or orange throat and infralabials typical of the northern race, not enough material had been analysed to make a taxonomic decision. Branch (1998) acknowledged T. s. ansorgii as a "poorly defined" race, with the accompanying distribution map showing the two subspecies occurring parapatrically in the Kaokoveld region of north-western Namibia, but the extent of the species' range into Angola was not addressed. Material collected by Ceríaco et al. (2016b) from Namibe Province, Angola, including Leba Pass on the border with Huila, was preliminarily integrated into the dataset from Portik et al. (2011), and no significant difference from the nominotypical form was found, leading the authors to recognise T. sulcata as a monotypic species. Recent revisions of Angolan herpetofauna have conservatively treated ansorgii either as a synonym of sulcata (Marques et al. 2018) or as a subspecies (Baptista et al. 2019; Branch et al. 2019; Butler et al. 2019; Conradie et al. 2022). However, a recent comprehensive review of all Angolan *Trachylepis* taxa recognised *T. ansorgii* as a distinct species (Ceríaco et al. 2024) despite its cryptic morphology.

Here, we incorporate new genetic samples from Angola and Namibia with published sequences from Namibia and South Africa to generate a more complete dataset that covers the full representation of diversity within *T. sulcata sensu lato*. We aim to assess phylogenetic relationships and genetic structuring using tree-based and non-tree-based molecular methods, identify and evaluate the role of potential phylogeographic barriers that have shaped the taxon's current distribution in south-west Africa, and validate the taxonomic status and geographic boundaries of *T. ansorgii* and *T. sulcata* across their distributions in south-west Africa.

Materials and Methods

Sampling

New specimens were collected from Angola for this study, euthanised following an approved IACUC protocol (Villanova University #1866), preserved in 10% buffered formalin in the field, and transferred to 70% ethanol for storage. Liver tissue was removed before formalin fixation and preserved in RNALater and transferred to 95% ethanol for long term storage. Specimens were deposited in the herpetological collections of the California Academy of Sciences (CAS), San Francisco, USA; Museu Nacional de História Natural e da Ciência, Universidade de Lisboa (MUHNAC), Lisboa, Portugal; Museu de História Natural e da Ciência da Universidade do Porto (MHNCUP), Porto, Portugal; and Instituto Nacional da Biodiversidade e Áreas de Conservação (INBAC), Luanda, Angola.

A total of 124 ingroup samples were obtained for this study. Samples span the entirety of the known range of *T. sulcata* and *T. ansorgii*, including 29 samples from South Africa, 46 from Namibia, and 49 from Angola. Of these, 48 specimens from Namibia and South Africa were used in previous studies on the group (Portik et al. 2010, 2011). Importantly, topotypical material of *T. ansorgii* was collected and included from Caconda, Huila Province, Angola. In addition, various congeneric samples were included as outgroup taxa for rooting purposes in phylogenetic analyses. A list of samples used in this study, including accession numbers and locality data, is provided in Appendix Table A1.

Sequence Acquisition and Processing

Genomic DNA was extracted from preserved tissues using a salt-extraction protocol modified from Aljanabi and Martinez (1997). Polymerase Chain Reaction (PCR) amplification was performed for two mitochondrial loci (16S and ND2) and three nuclear loci (RAG1, MXRA5, EXPH5) based on their effectiveness in similar studies on *Trachylepis* taxa (Portik et al. 2010; Portik and Bauer 2012; Sindaco et al. 2012; Ceríaco et al. 2016a; Allen et al. 2017, 2019; Weinell and Bauer 2018; Marques et al. 2019). Primer pairs were taken from published studies (Palumbi et al. 1991; Macey et al. 1997; Portik et al. 2010; Portik and Bauer 2012). PCRs were run with negative controls and products were visualised using gel electrophoresis. Successful PCR reactions were cleaned using magnetic Serapure beads and ethanol rinses. After sequencing reactions with BigDye Terminator

and an additional bead-cleaning protocol, sequencing was performed on ABI 3730xl and 3130xl sequencers at Villanova University.

Sequence editing was manually performed in Geneious v11.0.2 to review correct base calling and identify heterozygous sites in nuclear loci. Protein coding sequences were translated to check for correct reading frames and premature stop codons. Alignments were created using the Geneious alignment option under default settings. All new sequences are available in the GenBank repository, with accession numbers listed in Table A1.

Phylogenetic Analyses

Maximum likelihood (ML) phylogenetic analyses were performed using RAxML v8.2.12 (Stamatakis 2014) on eight datasets: five individual loci (16S, ND2, RAG1, EXPH5, and MXRA5), a concatenated mitochondrial dataset (mito), a concatenated nuclear dataset (nuc), and a concatenated dataset of all five loci (all5). Individual gene trees for nuclear loci were run with the phased haplotypes to account for heterozygosity (PHASE v2.1; Stephens et al. 2001; Stephens and Donnelly 2003), while the concatenated nuc and all5 analyses used the unphased sequences. PartitionFinder2 (Lanfear et al. 2017) was used to determine the best partitions for codon positions in the gene trees, and for determining both gene and codon partitions in the concatenated datasets. The GTRGAMMA model was used for all partitions, as RAxML has limited model selection. Each run was called with the '-f a' option to compute 500 rapid bootstraps and search the best-scoring ML tree in a single run. Trees were visualised in FigTree v1.4.3 and manually rooted using the outgroup clade (affinis (maculilabris + notabilis)) (Weinell et al. 2019). Rapid bootstrap (BS) values greater than 70% and 95% were considered to represent 'supported' and 'highly supported' nodes, respectively.

Bayesian Inference (BI) was used to infer phylogenetic relationships for the mito, nuc, and all5 datasets. Partitions and models of evolution were determined in PartitionFinder2 using BIC criteria for model selection. MrBayes v3.2.2 (Ronquist et al. 2012) on the CIPRES platform v3.3 (Miller et al. 2010) was used to run Bayesian analyses, each consisting of two runs with four chains (three hot and one cold), and run for 20 million Markov chain Monte Carlo (MCMC) generations, sampling every 2 000 generations. Convergence was assessed using ESS scores (>200) and visualised in Tracer v1.7.1 with a 10% burn-in. Trees were visualised in FigTree v.1.4.3 and manually rooted using the (affinis, (maculilabris, notabilis)) clade (Weinell et al. 2019). Posterior Probability (PP) values greater than 0.95 were considered as evidence of strong support for nodal values.

Divergence Dating

A time-calibrated tree for the group was estimated using the mito dataset in BEAST v2.5.1 (Bouckaert et al. 2019). A single partition with the HKY+G substitution model was found to be optimal using BIC in PartitionFinder2. The 16S and ND2 genes were assigned separate uncorrelated lognormal clock models. A lack of relevant material prevented the use of fossil calibrations, so substitution rates were calibrated using published rates of both 16S and ND2 from the literature (Barley et al. 2015). Specifically, a normally distributed prior on the lognormal clock mean was

implemented on each gene, with ucldMean = 0.00895 and Sigma = 0.0025. This corresponds to a rate distribution of 0.48–1.31% Myr⁻¹, which encompasses the known mitochondrial substitution rates estimated for several reptile groups, including skinks. The same rate distribution for mitochondrial genes has been used to time-calibrate divergences in other *Trachylepis* studies (Karin et al. 2016; Allen et al. 2019). A coalescent tree prior with constant population size was chosen, given the close phylogenetic relationships of the ingroup and the dense population-level sampling. All other priors were left at default settings. The MCMC chain was run for 80 million generations, sampling every 8 000 generations. Convergence was analysed in Tracer v1.7.1, determined by ESS > 200 for each parameter. TreeAnnotator v2.5.1 was used to create a maximum clade credibility tree, discarding the initial 10% as burn-in. The resulting tree was visualised in FigTree v1.4.3.

Population Structure

Haplotype networks were constructed from each of the phased nuclear haplotypes (RAG1, EXPH5, and MXRA5) using the TCS network inference method (Clement et al. 2002) implemented in PopArt v1.7 (Leigh and Bryant 2015). Trait blocks were uploaded to visualise the networks with the colours of different haplogroups reflecting mitochondrial clades.

Population delimitation was determined with the program STRUCTURE v2.3.4 (Pritchard et al. 2000) using a concatenated dataset of the phased nuclear data stripped of conserved sites. Individuals were assigned to one of 14 putative populations (K = 1-14) determined by geographic clustering and mitochondrial clades. The linkage model setting was used to map distances between loci, given that Single Nucleotide Polymorphisms (SNPs) within the same marker likely share an evolutionary history. The program ran for 100 000 MCMC repetitions after a burn-in of 100 000 repetitions for 10 iterations per K value. The Evanno method criterion (Evanno et al. 2005) implemented in StructureHarvester (Earl and von Holdt 2012) was utilised to choose the optimal K value. Results were combined and visualised using CLUMPP v1.1.2 (Jakobsson and Rosenberg 2007) and DISTRUCT v1.1 (Rosenberg 2004).

To infer intra- and inter-population dynamics, various statistics and tests were run in Arlequin v3.1 (Excoffier et al. 2005). Individuals were assigned to one of seven populations based on clades recovered in the phylogenetic analyses. Five datasets were analysed for each clade: mito, RAG1, EXPH5, MXRA5, and nuc. To analyse intra-population dynamics, nucleotide diversity (π), within population pairwise differences (k), Tajima's D, and Fu's Fs values were calculated for all five datasets. For inter-population dynamics, pairwise fixation indices (F_{ST}) were calculated. In addition, several Analyses of Molecular Variance (AMOVA) were performed to test four different biogeographic scenarios: 1) a three-species scenario (northern, central, and southern); 2) a two-species scenario with the division in northern Namibia; 3) a two-species scenario with the division in south-western Angola; and 4) a two-species scenario with the division at the Kunene River comparing Angolan vs. Namibian samples (Supplementary Material Figure S1). Each model was run separately for the mito and nuc datasets, using uncorrected pairwise distances and 5 000 random permutations.



Results

Phylogenetics

Except for the ND2 tree, individual gene trees of both mitochondrial and nuclear loci generally show little structure and are characterised by low support (Figures S1-S6). The concatenated mito phylogenies of both ML and BI analyses recover seven distinct subclades with good support, although several internal nodes lack support (Figure 1; Figures S7–S8). The subclades generally reflect geographic population structure, with four of the seven pertaining to Angola (Pop1-4), two in northern Namibia (Pop5-6), and one large subclade extending from central Namibia across western South Africa (Pop7). The seven populations comprise two main clades: a northern clade restricted to Angola composed of Pop1 and Pop2, and a southern clade spanning from southern Angola to South Africa composed of Populations 3-7. While this southern clade showed good support in the BI tree (0.98 PP), it was recovered with low bootstrap support (67) in the ML tree. Topotypical material of T. ansorgii was recovered in Pop2 of the northern clade, while neartopotypical material of T. sulcata (MCZR 193268 from vic. Okahandja, ~21 km NE of type locality, Gross Barmen) was recovered in Pop7 of the southern clade. The individual from Epupa Falls (MCZ R190247) on the Namibian/Angolan border consistently groups with Pop2 from Angola, despite being over 200 km to the south of other individuals in this clade.

The concatenated all5 analyses show similar results to the mito phylogenies in both ML and BI approaches (Figure 2, Figure S9). Each of the seven subclades comprising the two main clades were recovered with good support, except for Pop1 and Pop2 in the T. ansorqii clade, which were not recovered as reciprocally monophyletic in the combined dataset. The two south-western Angolan clades (Pop3 and Pop4) were recovered as sister to each other and together are sister to the three southern populations (Pop5-7).

The time-calibrated BEAST tree from the mito dataset (Figure 3) recovered nearly the same topology as the ML and BI mito trees. The relative relationships of Pop3, Pop4, and Pop5 differ between the trees, and these received low nodal support in all analyses. The clock rate for 16S was found to be 0.50% Myr⁻¹ (0.25–0.80 95% highest posterior distribution, HPD), while the ND2 clock was estimated to be 1.12% Myr⁻¹ (0.69-1.55 95% HPD). The root age of the clade (i.e., the split between the northern populations and the rest of the clade) corresponds to the late Miocene/early Pliocene (5.87 mya, 95% HPD 3.70-9.25). Further population-level splits were found in the Plio-Pleistocene (Figure 3).

Population Structure

Haplotype networks of the three phased nuclear loci (Figure 4) reflect geographic population clustering observed in the phylogenetic analyses. Overall, a clear distinction is seen between the northern grouping (Pop1 and Pop2) and the southern grouping (Pop5-7). The central grouping (Pop3 and Pop4) shows affinity with northern populations in the RAG1 network, southern populations in the MXRA5 network, or split in the case of the EXPH5 network in which Pop4 groups near the northern populations but Pop 3 shows affinity for the southern populations. The distinctiveness between the two northern

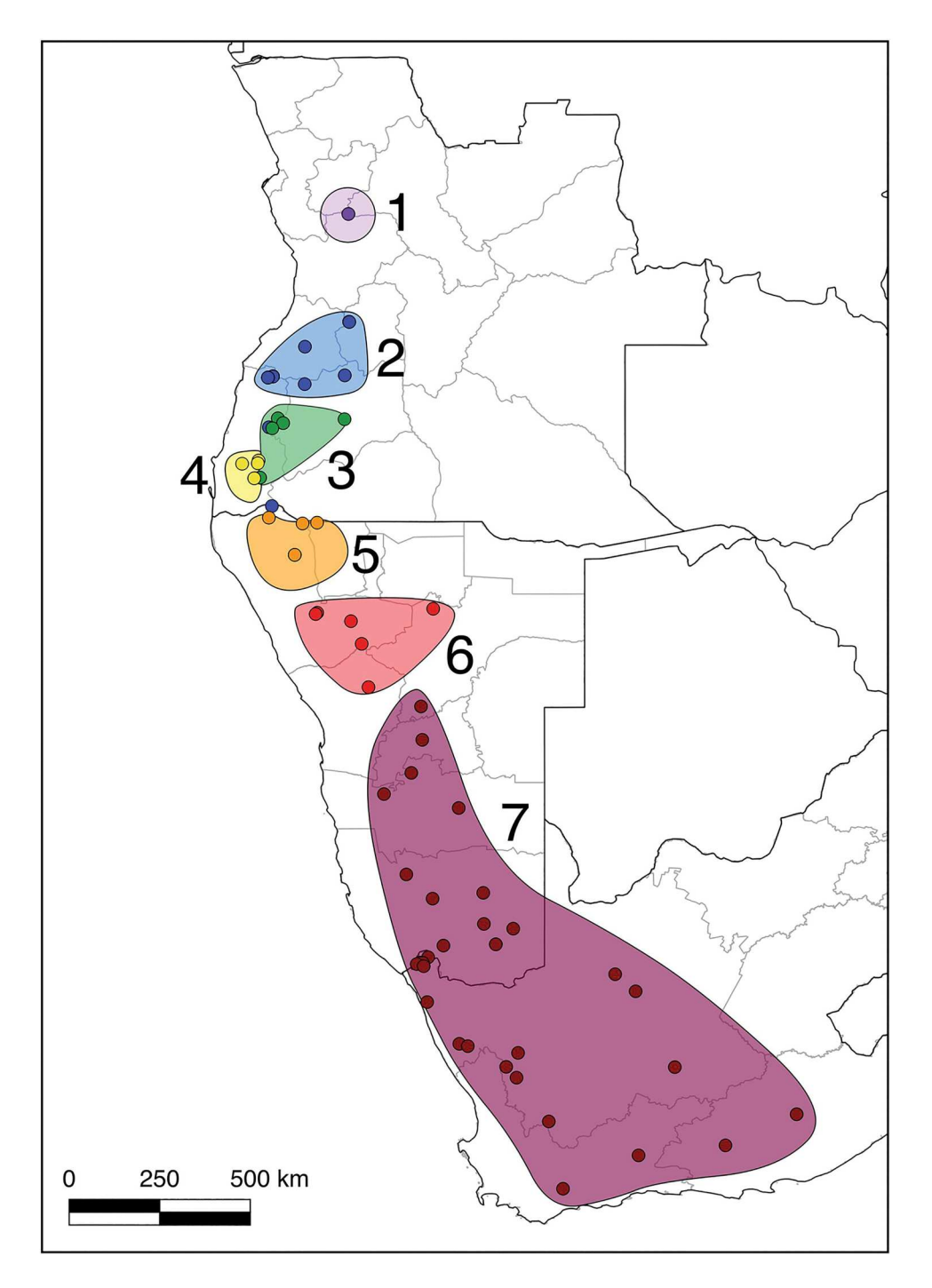


Figure 1: Sampling localities for the analysed dataset of the *Trachylepis sulcata* complex, coloured by mitochondrial clade identity. Colours are consistent across the figures in this manuscript.

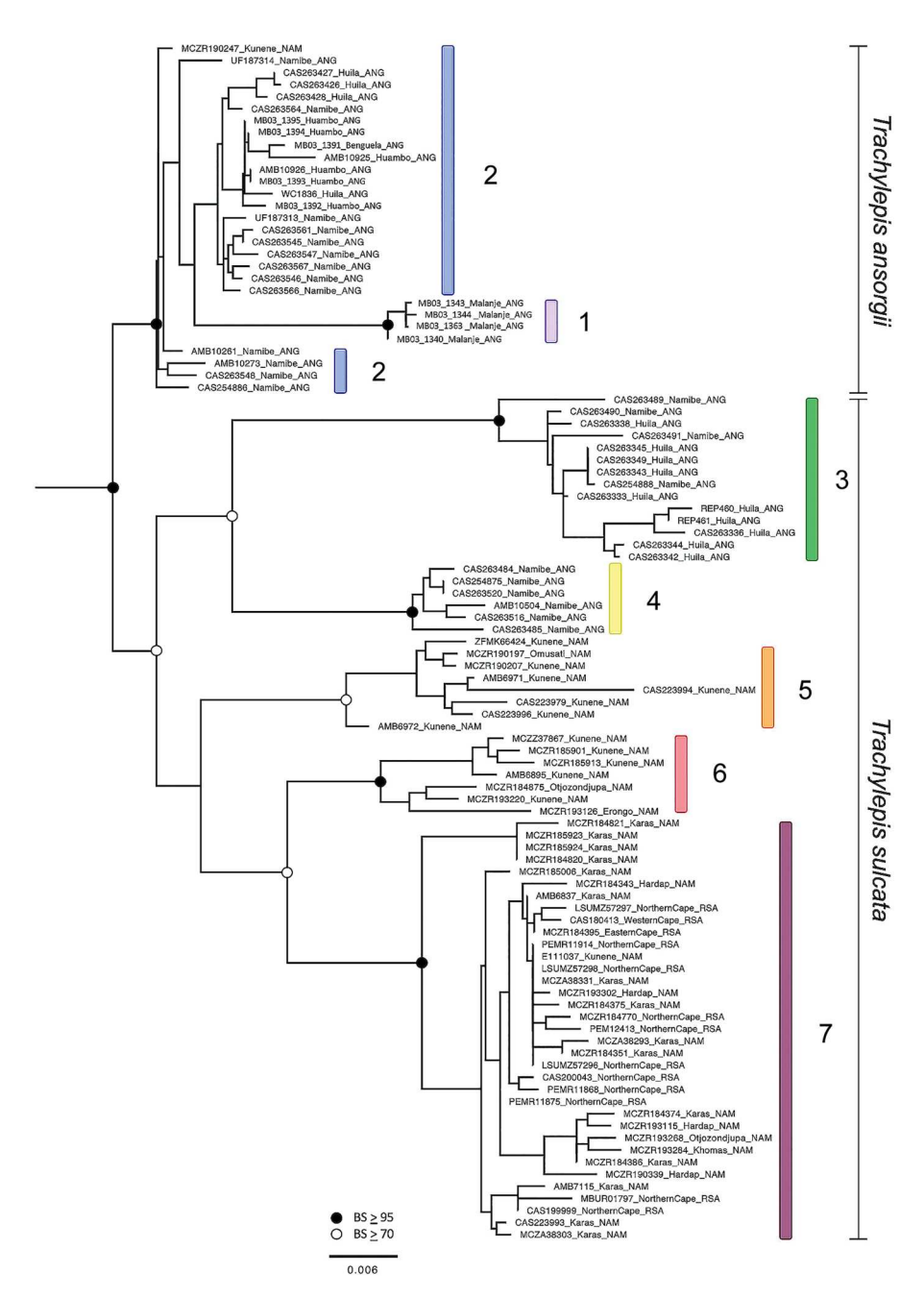


Figure 2: RAxML tree of the unphased concatenated dataset (*all5*), with nodes supported (bootstrap > 70) and highly supported (bootstrap > 95) in white and black circles, respectively. Outgroup taxa are not shown. Ingroup taxa are coloured by mitochondrial groupings (*mito*).

populations (Pop1 and Pop2) is only observed in the EXPH5 network, whereas in the RAG1 and MXRA5 networks these two northern mitochondrial clades share nuclear haplotypes. In general, the three southern mitochondrial clades (Pop5–7) show shared or highly similar nuclear haplotypes. The MXRA5 network is the only one that presents a shared

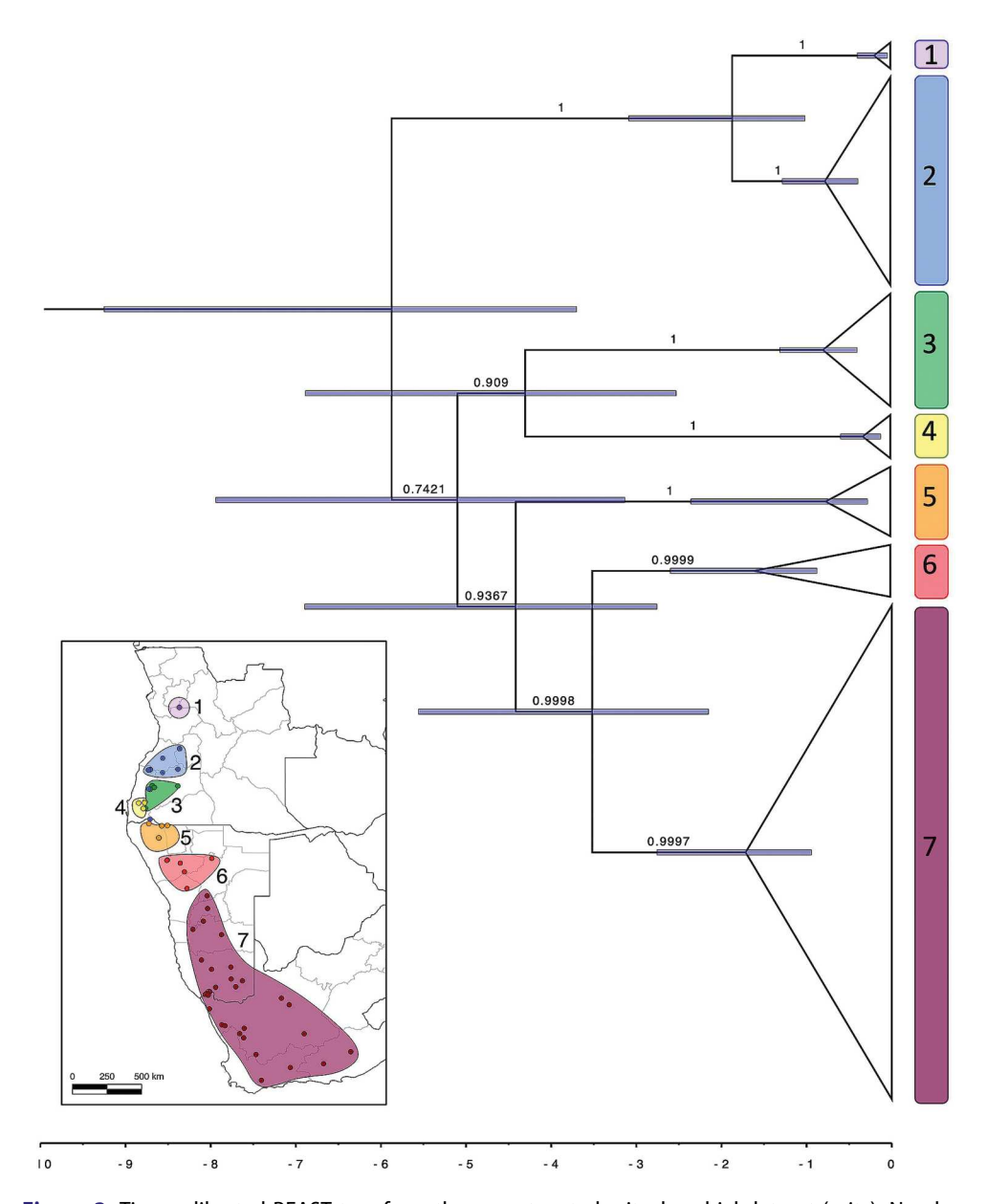


Figure 3: Time-calibrated BEAST tree from the concatenated mitochondrial dataset (mito). Numbers on branches represent Posterior Probabilities, whilst bars at nodes represent the 95% highest posterior distribution (HPD) intervals of divergence dates, scaled in millions of years before present. Coloured rectangles and clade numbers correspond to mitochondrial clade identities, shown in the inset map of sampling localities.

nuclear haplotype between a northern (Pop2) and southern (Pop6) mitochondrial clade, as well as a central (Pop4) mitochondrial clade.

The concatenated phased nuclear dataset input into STRUCTURE included 106 individuals with 254 variable loci. A population structure of K=3 was best supported by the model ($\Delta K = 12.09$), followed by K = 4 ($\Delta K = 10.47$) (Figure S10). The ancestry bar plot

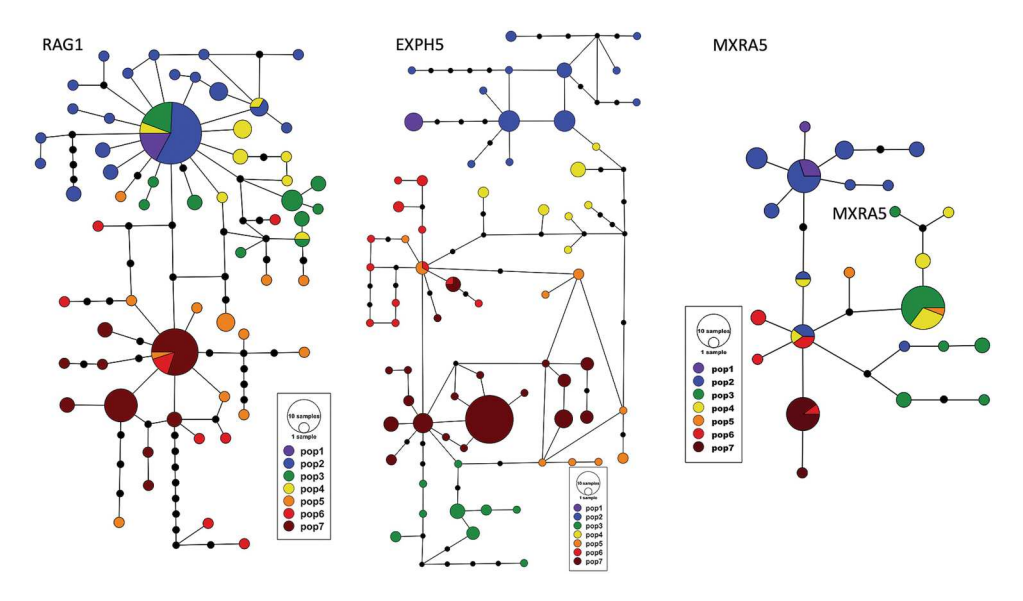


Figure 4: Haplotype networks of the three phased nuclear loci. Circle size represents number of individuals, while colours correspond to mitochondrial groupings.

with the three groupings and their comparison to mitochondrial populations is shown in Figure 5. A northern grouping (blue bar plots) contains homogenous individuals in northern Namibe and Huíla provinces to Malanje, Angola (~9–14°S), corresponding to *T. ansorgii*. The central grouping (yellow bar plots) contains a few individuals with complete ancestry assigned to this central grouping but is mainly composed of admixed individuals showing shared ancestry with either the northern or southern groups. Northcentral admixed individuals are from south-western Angola south to the Kunene River border with Namibia (mitochondrial Pop3 and Pop4, ~14°–17°S), and south-central individuals are found from the Kunene River south to central Namibia (mitochondrial Pop5 and Pop6, ~17° to 20°S). The southern grouping (red bar plots) includes individuals from South Africa to central Namibia (mitochondrial Pop7).

Genetic diversity at the population level was found to be the highest in Pop6 from central Namibia for mtDNA (Table S1; π = 0.012506; k = 19.81). For nuclear data, Pop4 from Namibe, Angola had the highest diversity (Table S1; π = 0.005997; k = 17.67). Several populations showed significantly negative neutrality tests. For Tajima's D, this was observed in the mtDNA for Pop3, Pop4, Pop5, and Pop7; and in the nDNA for Pop1 and Pop2 (Table S1). For Fu's Fs, this was observed in the mtDNA for Pop2, Pop3, Pop5, and Pop7; and in the nDNA for all populations except Pop4.

Pairwise F_{ST} values using the nuclear data are centred around 0.5 in the 7-population model (Figure 6A), suggesting intermediate gene flow between nearby populations. The highest pairwise F_{ST} value was found between the most geographically separated populations, Pop1 and Pop7 (0.788), while the lowest nuclear F_{ST} value was between Pop5 and Pop6 (0.224). The 3-population model with the nuclear data produced similar results (Figure 6B), with the highest value (0.649) between the central and southern groupings. The central grouping showed similar F_{ST} values when analysed with the northern grouping (0.365) as with the southern grouping (0.392). The mitochondrial data showed overall

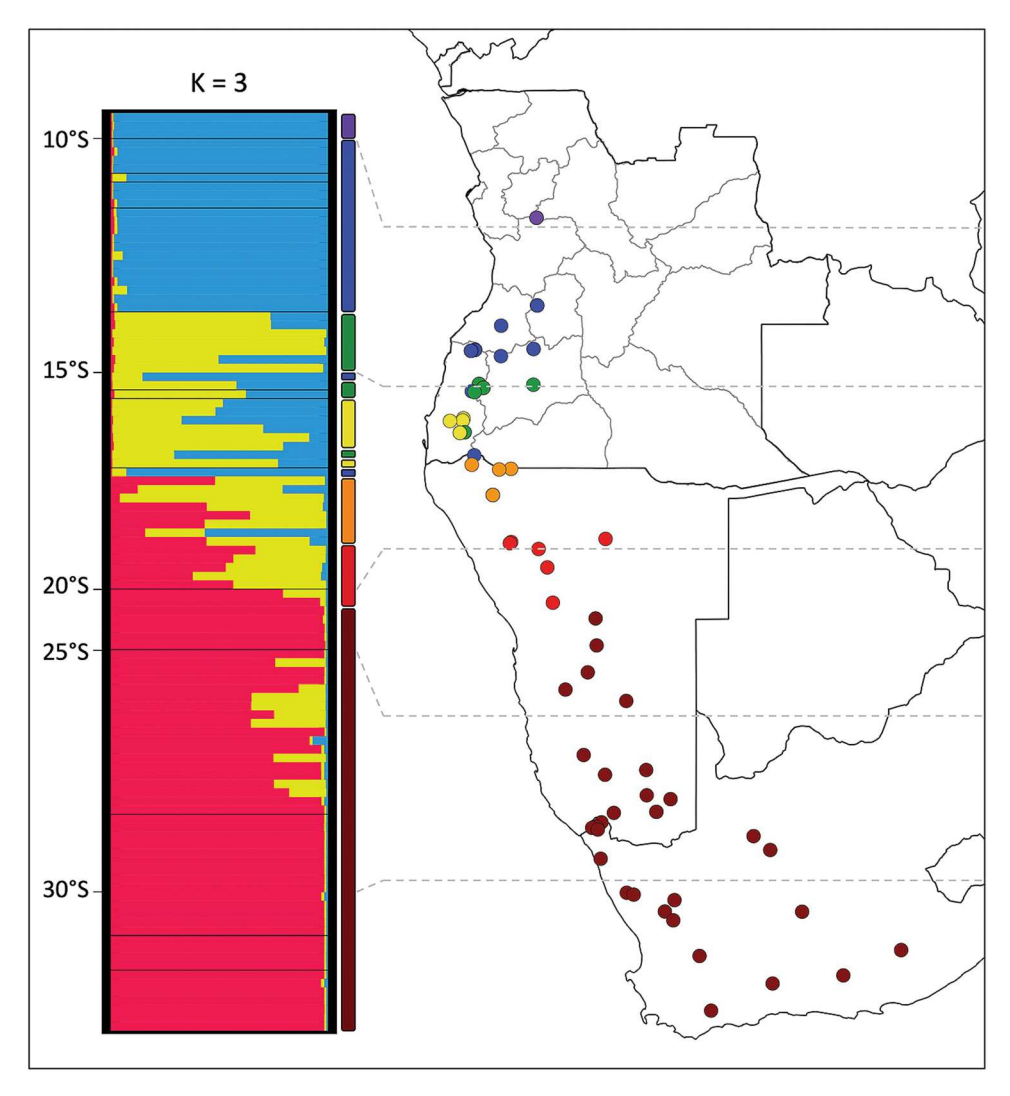


Figure 5: Structure plot (left) organised with individuals arranged by latitude (north to south). Mitochondrial population grouping is denoted by thin rectangular bars to the right of larger plot. Map of samples included in STRUCTURE analysis (right) with samples coloured by mitochondrial grouping.

higher pairwise F_{ST} values between populations, as expected. In the 7-population model (Figure 6A), Pop1 and Pop4 showed the highest genetic isolation ($F_{ST} = 0.936$), while Pop6 and Pop7 showed the lowest ($F_{ST} = 0.759$). Similar to the nuclear data, the mitochondrial data in the 3-population model showed the highest differentiation between the northern and southern groupings (Figure 6B; $F_{ST} = 0.773$). The central grouping was found to have a slightly lower F_{ST} value when compared to the southern grouping than to the northern grouping (0.529 and 0.615, respectively).

Among the four scenarios tested with the AMOVA using the mitochondrial dataset, the highest proportion of explained genetic variance among groups was found in the twospecies scenario that grouped the central populations (Pop3 and Pop4) with the southern

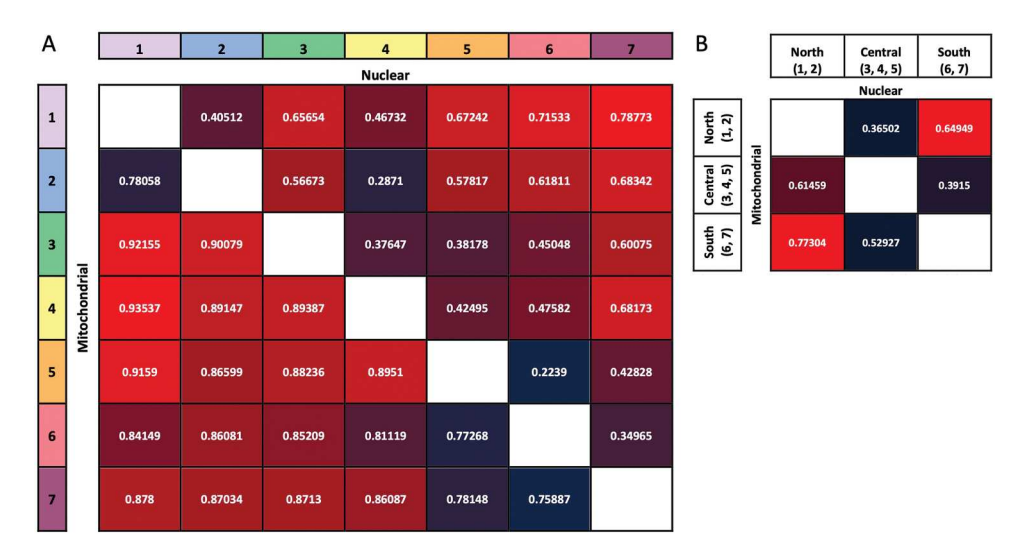


Figure 6: F_{ST} heatmaps for A) 7-population model and B) 3-population model. Nuclear values are above the diagonal and mitochondrial values below the diagonal. Higher relative F_{ST} values are red, while lower relative values are dark blue. Population numbers refer to mitochondrial clades.

populations (Populations 5–7), showing their division in south-western Angola (Va = 10.118; Table 1). This variation explained 26.72% of the total genetic variation found in the mitochondrial dataset. The two-species scenario that groups the central populations with the northern populations (Pop1 and Pop2) produced a negative Va (-1.433), suggesting that this scenario with a division in northern Namibia is not representative of the data. The AMOVAs for the nuclear dataset showed different results, with the two-species scenario with a division at the Kunene River showing the highest Va at 3.114, representing 31.11% of total genetic variation in the dataset. The second highest proportional variation among groups for both mito and nuc datasets was the threespecies scenario. For all four scenarios, the largest source of variation was within populations (Table 1).

Discussion

Although previous work has revealed aspects of the phylogeographic history of Trachylepis sulcata in south-western Africa (Portik 2009; Portik et al. 2010, 2011), incomplete sampling in Angola precluded a comprehensive evaluation and a taxonomic assessment of T. sulcata and T. ansorgii across south-western Africa. With the inclusion of populationlevel Angolan sampling for the first time, this study fills a large gap in our understanding of these widespread south-western African skinks.

Phylogenetic and population genetic results are largely congruent regarding population structuring within Trachylepis sulcata sensu lato, recovering at least two distinct major evolutionary lineages. The ML nuc phylogenetic tree recovers, albeit with low support, a sister relationship between a mostly Angolan clade and a Namibian/South African clade. The mitochondrial data found support for seven populations also comprising two major clades. The higher level of structure revealed by the mitochondrial DNA

(<u>-</u>

constituting a central group (top row); two distinct groups with the division in north-west Namibia (second row); two distinct groups with the division at the Cunene River (bottom row). Numbers next to clade divisions refer to **Table 1:** AMOVA results from the mitochondrial (mito; left) and nuclear (nuc; right) datasets. Different hypotheses for group assignments were tested based on phylogenetic results (see Supplementary Figure S1): three distinct groups, with the southern Angolan and northern Namibian populations (Pops 3, 4, 5) mitochondrial clades (see Figure 1).

		Mitochondria	ndrial					Nuclear	ır		
		Three clades: (1,	(1,2) (3,4,5) (6,7)					Three clades (1,2) (3,4,5) (6,7)	(3,4,5) (6,7)		
Source of variation	d.f.	Sum of Squares	Variance	% var.	Fixation	Source of variation	d.f.	Sum of Squares	Variance	% var.	Fixation Indices
Among groups	72	1642.1	6.8 Va	20.1	F _{cr} = 0.83	Among groups	7	611.3	2.8 Va	30.2	$F_{cc} = 0.42$
Among pops	4	864.3	22.5 Vb	66.5	$F_{ST} = 0.86$	Among pops	4	198.8	2.8 Vb	29.4	$F_{ST} = 0.60$
within groups Within pops	116	526.5	4.5 Vc	13.4	$F_{CT} = 0.20$	within groups Within pops	205	778.0	3.8 Vc	40.0	$F_{CT} = 0.30$
•		1	1	10.04		i				1	
	o clade	I wo clades: (1,2,3,4,5) (6,7) —	north-west Namibia divide	bia divide	i		o clade:		nortn-west Namibia divide	bia divide	į
Source of	д. Т	Sum of Squares	Variance	% var.	Fixation	Source of	д.	Sum of Squares	Variance	% var.	Fixation
variation			components		Indices	variation			components		Indices
Among groups	-	898.1	-1.4 Va	4.4	$F_{SC} = 0.87$	Among groups	-	444.4	2.2 Va	23.1	$F_{SC} = 0.49$
Among pops	2	1608.3	29.3 Vb	90.4	$F_{ST} = 0.86$	Among pops	2	365.6	3.6 Vb	37.6	$F_{ST} = 0.61$
within groups	;	;	:	;	;	within groups	;	İ		;	
Within pops	116	526.5	4.5 Vc	14.0	$F_{CT} = -0.04$	Within pops	202	778.0	3.8 Vc	39.3	$F_{CT} = 0.23$
≱ ⊢	vo clado	Two clades: (1,2) (3,4,5,6,7) —	- south-west Angola divide	ola divide		Ž	o clade	Two clades: (1,2) (3,4,5,6,7) —	south-west Angola divide	ola divide	
Source of	d.f.	Sum of Sauares	Variance	% var.	Fixation	Source of	d.f.	Sum of Sauares	Variance	% var.	Fixation
doiteirex			Components		Indices	variation		-	Componente		Indicae
Among ground	,	0.6301	10.1 %	7.90		Among ground	-	C 1/2	25 1/2	3 1/5	
sdporg ground	- '	0.2001	10.1 va	70.7	- SC - 0:01	sdpoile gironin	- '	2.4.0	2.7 va	C.+.2	
Among pops	2	1444.5	23.2 Vb	61.3	$F_{ST} = 0.88$	Among pops	2	435.8	3.9 Vb	38.4	$F_{ST} = 0.63$
within groups Within pops	116	5765	4 5 Vc	12.0	F ₋₇ = -0.27	within groups Within pops	205	778.0	38 Vc	37.7	$F_{c7} = 0.24$
	-		2	i	ì		2			!	!
	Two cl	Two clades: (1,2,3,4) (5,6,7)) — Cunene River divide	divide			Two cla	Two clades: (1,2,3,4) (5,6,7)	— Cunene River divide	divide	
Source of	d.f.	d.f. Sum of Squares	Variance	% var.	Fixation	Source of	d.f.	Sum of Squares	Variance	% var.	Fixation
variation			components		Indices	variation			components		Indices
Among groups	_	970.6	2.0 Va	6.1	$F_{SC} = 0.84$	Among groups	_	475.2	3.1 Va	31.1	$F_{SC} = 0.45$
Among pops	2	1585.9	27.0 Vb	80.4	$F_{ST} = 0.88$	Among pops	2	334.9	3.1 Vb	31.0	$F_{ST} = 0.62$
within groups						within groups					
Within pops	116	526.5	4.5 Vc	12.0	$F_{CT} = -0.27$	Within pops	205	778.0	3.8 Vc	37.9	$F_{CT} = 0.31$

(mtDNA) is expected and reflects more recent evolutionary history given the inherent properties of mtDNA. The concatenated all5 trees show topologies similar to the mito trees, except for the lack of differentiation between the two northern populations (Pop1 and Pop2). While southern Namibia and South Africa constitute nearly half of the area of distribution for these skinks, only one of seven populations is found in this region. Most of the diversity is recovered in south-western Angola and north-western Namibia.

The geographic boundary between the T. ansorgii and T. sulcata clades is of particular interest. Depending on the analysis, the south-west Angolan populations (Pop3 and Pop4) are recovered as either: 1) sister to the northern populations (Pop1 and Pop2) forming a mostly Angolan clade (nuc AMOVA, Table 1; nuc ML tree, Figure S11); 2) sister to the southern populations (all5 ML and BI trees, Figure 2, Figure S8; mito AMOVA, Table 1); or 3) as a distinct evolutionary unit combined with the northern Namibian population (Pop5) (STRUCTURE plot, Figure 5). Nodal support values for these clades were consistently low across analyses, highlighting the uncertainty of their phylogenetic placement. The phased nuclear haplotype networks also show varying relationships where these central populations either group with the northern populations (RAG1), are intermediate between northern and southern (MXRA5), or are split between showing northern and southern haplotypic affinities (EXPH5) (Figure 4).

Taken together, these results support the recognition of two evolutionarily distinct lineages with a zone of introgression in south-western Angola/north-western Namibia. This is best seen in the STRUCTURE plot of the nuclear dataset (Figure 5), in which the central grouping (yellow barplots) contains nearly all admixed individuals with either the northern T. ansorqii haplotype (blue, ~14 to 17°S) or the southern T. sulcata haplotype (red, ~17 to 20°S, with some additional shared ancestry individuals in southern Namibia, ~27°S). This division between 'central/northern' and 'central/southern' shared ancestry individuals at 17°S corresponds with the Kunene River and the political boundary between Angola and Namibia. While there are no haplotypes of the southern T. sulcata cluster (red) extending into Angola, a few individuals with the northern T. ansorgii haplotypes (blue) are found in Namibia (Figure 5).

The lack of available Angolan samples in previous studies on T. sulcata (Portik 2009; Portik et al. 2010, 2011) provides an interesting comparison with this study. The two datasets are concordant in finding the highest level of genetic diversity in the northern part of the species' range, although the additional sampling provided in this study shifted that centre of genetic diversity from north-western Namibia to south-western Angola. The three mitochondrial clades recovered in Portik (2009) from the ND2 locus were also recovered in this study (Pop5, Pop6, Pop7), with the addition of four more mitochondrial clades in Angola (Pop1-4). The nuclear break reported in the Knersvlakte region in western South Africa by Portik (2009) and Portik et al. (2011) was not recovered in the present study (Figure 5). The inclusion of T. ansorgii in this study increased levels of genetic diversity relative to the previous study (Portik et al. 2011), making the relatively low amount of variation responsible for the previously identified Knersvlakte break less significant overall. Interestingly, mito-nuclear discordance was found in both studies, although in different geographic regions (Western Cape province, South Africa in Portik et al. 2011, south-western Angola in this study).

The time-calibrated mito tree estimated the root age for T. sulcata sensu lato in the Late Miocene, ~6 mya, when the two major lineages of *T. sulcata* and *T. ansorgii* diverged (Figure 3). This date is consistent with the findings in the genus-level phylogeny (Weinell et al. 2019) that utilised a secondary calibration for the crown age of Mabuyinae taken from the time-calibrated Squamata phylogeny of Zheng and Weins (2016). Within the genus Trachylepis, many pairs of sister-taxa diverged in the Late Miocene/Pliocene around the same time as T. sulcata and T. ansorgii (Weinell et al. 2019). Within T. ansorgii, a Pleistocene divergence was recovered in the mtDNA between Pop1 and Pop2, although the nDNA did not recover the two clades as distinct. Lineage splitting for the remainder of the group occurred during the Pliocene, followed by a Pleistocene expansion of T. sulcata across southern Namibia and South Africa, as previously hypothesised (Portik et al. 2011).

Although the geographic delimitation between the two sister species differs among data types, cytonuclear discordance can often inform evolutionary histories (Toews and Brelsford 2012). The division inferred from the slowly evolving nuclear data aligns with the Kunene River, suggesting the importance of this hydrological feature in the early isolation between T. sulcata and T. ansorgii. A river capture event that connected the upper and lower segments of the Kunene River is hypothesised to have occurred between 2.5-5 mya (Hipondoka 2005; Hoetzel et al. 2015). The Late Pliocene split between T. sulcata and T. ansorgii found in this study with the mito dated phylogeny supports the timing of the Kunene River capture around the Miocene-Pliocene transition, described in Hoetzel et al. (2015) at \sim 5 mya. While the divergence is slightly older than this, a proto-Kunene River existed prior to the river capture date, as present-day hydrological patterns along the Great Escarpment suggest river incisions formed throughout the Great Escarpment (Partridge and Maud 1987). This may explain the nuclear differentiation between northern and southern clades observed at the Kunene River. The more rapidly evolving mitochondrial data show the division between T. ansorgii and T. sulcata to be \sim 250 km north of the Kunene River, with southwestern Angolan populations (Pop3 and Pop4) showing greater affinity to T. sulcata from across the Kunene River in Namibia, suggesting a mitochondrial introgression northward into southern Namibe and Huíla provinces in Angola. The presence of outlier taxa being recovered in clades not corresponding with their geographic location (i.e., MCZ R190247, AMB 6972) in both nuclear and mitochondrial trees implies some level of gene flow between major clades, potentially from recent human-mediated accidental translocations. Evolutionary processes that have been invoked to explain conflicting patterns between mitochondrial and nuclear data in other taxa include introgressive hybridisation, sex-based dispersal, independent lineage sorting, and hybrid zone movement (Folt et al. 2019; Wielstra and Arntzen 2020; Marshall et al. 2021; Ambu et al. 2023; Burriel-Carranza et al. 2023). A comprehensive analysis of the skinks from this region of interest, including more extensive sampling, a detailed morphological assessment, and/or more loci (i.e., a genomic dataset) would help clarify the phylogenetic placement of the south-western Angolan populations, which are tentatively allocated here to T. sulcata.

The Angolan Great Escarpment, an abrupt elevational and climatic transition between the dry lowlands of Namibe Province and the Huíla Plateau and Serra da Chela mountain range, appears to act as a minor phylogeographic barrier. Specifically, this geologic feature divides the two south-western Angolan populations into above-escarpment (Pop3) and below-escarpment (Pop4) entities, with this division corresponding to ~600-750 m a.s.l. However, the relatively recent Pliocene divergence between these two populations (~4 mya) postdates known periods of orogenic uplift in the western Great Escarpment. More likely, environmental differences associated with a rapid elevational gradient reinforce observed population structuring. In contrast, lower elevational populations in Namibia and South Africa are not genetically distinct from their escarpment-dwelling counterparts (Portik et al. 2011).

The molecular results from this study are consistent with the recent taxonomic elevation of T. ansorgii to species-level, and the taxon's sister relationship with T. sulcata (Ceríaco et al. 2024). Concerted sampling efforts for populations in southwestern Angola, paired with previous studies on Namibian and South African material, offer a new insight into the population structuring, genetic divergence, and geographic boundaries in Trachylepis sulcata sensu lato across its entire distribution. However, the translation of genetic data into taxonomic allocations is not straightforward. The study here captures ongoing processes, such as the potential introgression of T. sulcata mitochondrial DNA into T. ansorgii and/or incomplete lineage sorting, hence the discrepancies in both the number of units present and the geographic division between them. These taxa have been recognised as distinct forms by at least some authorities for over 100 years and have valid names associated with them, even if the morphological characters used by these authors to support this recognition were, most of the time, vague or even contradictory. Indeed, they represent cryptic species that are very conservative in their morphologies, and they are difficult to tell apart without molecular data; however, the inclusion of topotypical genetic material in the present study for T. ansorgii and near-topotypical material for T. sulcata adds clarity to taxonomic allocations of populations. Furthermore, the divergence age between T. ansorgii and T. sulcata in the Late Miocene is concordant with species-level splits in other Trachylepis taxa (Weinell et al. 2019; Ceríaco et al. 2024). Based on our population-level results, T. ansorgii is endemic to the central Angolan escarpment and highlands region, while T. sulcata is recognised from South Africa and western Namibia. South-west Angolan populations south of 14°S are tentatively allocated to T. sulcata, but further studies from this region and northwestern Namibia are required to clarify the status of such populations. Our results raise the possibility of these populations representing a third species-level lineage, and future fieldwork from the sampling gap in Cunene Province, Angola will help resolve this issue.

Molecular methods have successfully recognised hidden species-level diversity in Trachylepis from oceanic islands (Sindaco et al. 2012; Ceríaco et al. 2016a), central Africa (Allen et al. 2017), southern Africa (Weinell and Bauer 2017), and Angola (Margues et al. 2019; Ceríaco et al. 2024). Additional field surveys will likely uncover further cryptic diversity within the genus. Despite being relatively under-explored compared to other southern African countries, Angola boasts the largest number of Trachylepis species at 25, including both *T. sulcata* and *T. ansorgii* (Ceríaco et al. 2024).

Several transitional ecotones are found within Angola, with the most prominent being that between the humid tropics and the arid deserts of southern Africa (Marques et al. 2018; Branch et al. 2019). Trachylepis ansorgii and T. sulcata reflect this transition, as their geographic boundaries correspond to the stark environmental gradients that drive habitat differentiation across a relatively small transect. The Huíla Plateau of the

Angolan Great Escarpment harbours high genetic diversity and likely has acted as a source of diversification for T. sulcata and T. ansorgii. These results highlight this escarpment's evolutionary importance in generating high levels of biodiversity and endemism across taxonomic groups. Current conservation areas do not adequately preserve such evolutionary unique assemblages persisting in the Angolan Great Escarpment (Clark et al. 2011), and future work to document the region's biodiversity is needed in order to promote conservation.

Acknowledgements

This paper is a result of BOB's MSc thesis at Villanova University, and he would like to thank his laboratory mates and the administrative staff of the Villanova Biology Department for their assistance. Special thanks go to Suzana Bandeira, Timóteo Júlio, Mariana Marques, and Matthew Heinicke for their help in the field and to Fernanda Lage and Francisco Maiato Gonçalves of the Instituto Superior de Ciências da Educação (ISCED) in Lubango for their institutional support during fieldwork. Fieldwork for this project was performed under collecting and export permits from Angola (155/INBAC.-MINAMB/2017; 28/INBAC.MINAMB/2019), Namibia (Namibian Ministry of Environment and Tourism Permit No. 098082 and earlier permits), and the Western and Northern Cape Provinces (series of permits issued to AMB 1987-2013). Funding was provided by U.S. National Science Foundation grants DEB 0515909, 1556255, 1657527, 2146654 to AMB.

Disclosure statement

No potential conflict of interest was reported by the author(s).

ORCID

Brett O Butler http://orcid.org/0000-0001-8617-8931 Luis MP Ceríaco http://orcid.org/0000-0002-0591-9978 *Aaron M Bauer* http://orcid.org/0000-0001-6839-8025

References

Aljanabi SM, Martinez I. 1997. Universal and rapid salt-extraction of high quality genomic DNA for PCR-based techniques. Nuc. Acids Res. 25(22): 4692–4693. https://doi.org/10.1093/nar/25.22. 4692.

Allen K, Tapondjou WP, Welton LJ, Bauer AM. 2017. A new species of Trachylepis (Squamata: Scincidae) from central Africa and a key to the Trachylepis of West and Central Africa. Zootaxa. 4268(2): 255–269. https://doi.org/10.11646/zootaxa.4268.2.5.

Allen KE, Tapondjou WP, Greenbaum E, Welton L, Bauer AM. 2019. High levels of phylogenetic structure within Central and West African Trachylepis skinks. Salamandra. 55(4): 231–241.

Ambu J, Martínez-Solano I, Suchan T, Hernandez A, Wielstra B, Crochet PA, Dufresnes C. 2023. Genomic phylogeography illuminates deep cyto-nuclear discordances in midwife toads (Alytes). Mol. Phylogenet. Evol. 183: 107783.https://doi.org/10.1016/j.ympev.2023.107783.

Baptista NL, António T, Branch WR. 2019. The herpetofauna of Bicuar National Park and surroundings, southwestern Angola: a preliminary checklist. Amphib. Reptile Conserv. 13(2): 96-130.

Barley AJ, Datta-Roy A, Karanth KP, Brown RM. 2015. Sun skink diversification across the Indian-Southeast Asian biogeographical interface. J. Biogeogr. 42(2): 292–304. https://doi.org/10.1111/ jbi.12397.

Bauer AM, Branch WR, Haacke WD. 1993. The herpetofauna of the Kamanjab area and adjacent Damaraland, Namibia. Madoqua. 18(2): 117–145.



- Bouckaert R, Vaughan TG, Barido-Sottani J, Duchêne S, Fourment M, Gavryushkina A, Heled J, Jones G, Kühnert D, De Maio N, et al. 2019. BEAST 2.5: An advanced software platform for Bayesian evolutionary analysis. PLoS Comput. Biol. 15(4): e1006650. https://doi.org/10.1371/journal.pcbi. 1006650.
- Boulenger GA. 1907. Descriptions of three new lizards and a frog, discovered by Dr. W. J. Ansorge in Angola, Ann. Mag. Nat. Hist. 19(111): 212–214. https://doi.org/10.1080/00222930709487258.
- Branch B. 1998. Field guide to the snakes and other reptiles of Southern Africa, 3rdedition. Cape Town: Struik, 368 p.
- Branch WR, Vaz Pinto P, Baptista N, Conradie W. 2019. The reptiles of Angola: history, diversity, endemism and hotspots. In: Huntley B, Russo V, Lages F, Ferrand N (eds.) Biodiversity of Angola. Springer, Cham. Xvii + 549 pp. https://doi.org/10.1007/978-3-030-03083-4 13.
- Burriel-Carranza B, Estarellas M, Riaño G, Talavera A, Tejero-Cicuéndez H, Els J, Carranza S. 2023. Species boundaries to the limit: Integrating species delimitation methods is critical to avoid taxonomic inflation in the case of the Hajar banded ground gecko (Trahcydactylus hajarensis). Mol. Phylogenet. Evol. 186: 107834.https://doi.org/10.1016/j.ympev.2023.107834.
- Butler BO, Ceríaco LMP, Marques MP, Bandeira S, Júlio T, Heinicke MP, Bauer AM. 2019. Herpetological survey of Huila Province, southwest Angola, including first records from Bicuar National Park, Herpetol, Rev. 50(2): 225-240.
- Ceríaco LMP, Margues MP, Bauer AM. 2016a. A review of the genus *Trachylepis* (Sauria: Scincidae) from the Gulf of Guinea, with descriptions of two new species in the Trachylepis maculilabris (Gray, 1845) species complex. Zootaxa. 4109(3): 284-314. https://doi.org/10.11646/zootaxa. 4109.3.2.
- Ceriaco LMP, dos Anjos Carlos de Sá S, Bandeira S, Valério H, Stanley E, Kuhn AL, Marques MP, Vindum JV, Blackburn DC, Bauer AM. 2016b. Herpetological survey of Iona National Park and Namibe Regional Natural Park, with a synoptic list of the amphibians and reptiles of Namibe Province, southwestern Angola. Proc. Calif. Acad. Sci. 63(2): 15-61.
- Ceríaco LMP, Marques MP, Parrinha D, Tiutenko A, Weinell JL, Butler BO, Bauer AM. 2024. The Trachylepis (Squamata: Scincidae) of Angola: an integrative taxonomic review with the description of seven new species. Bull. Am. Mus. Nat. Hist. No. 465. 153 p.
- Clark VR, Barker NP, Mucina L. 2011. The Great Escarpment of southern Africa: A new frontier for biodiversity exploration. Biodivers. Conserv. 20(12): 2543-2561. https://doi.org/10.1007/s10531-011-0103-3.
- Clement M, Snell Q, Walker P. 2002. TCS: Estimating gene genealogies. Proc. 16th Int. Parallel Distrib. Proc. Symp. p.184.
- Conradie W, Keates C, Verburgt L, Baptista NL, Harvey J, Júlio T, Neef G. 2022. Contributions to the herpetofauna of the Angolan Okavango-Cuando-Zambezi River drainages. Part 2: Lizards (Sauria), chelonians, and crocodiles. Amphib. Reptile Conse. 16(2): 181-214(e322).
- Daniels SR, Mouton P, Du Toit DA. 2004. Molecular data suggest that melanistic ectotherms at the south-western tip of Africa are the products of Miocene climatic events: evidence from cordylid lizards. J. Zool. 263(4): 373-383. https://doi.org/10.1017/S0952836904005424.
- Earl DA, vonHoldt BM. 2012. STRUCTURE HARVESTER: a website and program for visualizing STRUCTURE output and implementing the Evanno method. Conserv. Genet. Resour. 4(2): 359-361. https://doi.org/10.1007/s12686-011-9548-7.
- Engelbrecht, HM, Mouton PLFN, Daniels SR. 2011. Are melanistic populations of the Karoo girdled lizard, Karusasaurus polyzonus, relics or ecotypes? A molecular investigation. Afr. Zool. 46(1): 146– 155.https://doi.org/10.3377/004.046.0105.
- Evanno G, Regnaut S, Goudet J. 2005. Detecting the number of clusters of individuals using the software STRUCTURE: a simulation study. Mol. Ecol. 14: 2611-2620. https://doi.org/10.1111/j.1365-294X.2005.02553.x.
- Excoffier L, Laval G, Schneider S. 2005. Arlequin (version 3.0): An integrated software package for population genetics data analysis. Evol. Bioinform. Online. 1: 47–50. https://doi.org/10.1177/ 117693430500100003.
- Folt B, Bauder J, Spear S, Stevenson D, Hoffman M, Oaks JR, Wood Jr. PL, Jenkins C, Steen DA, Guyer C. 2019. Taxonomic and conservation implications of population genetic admixture, mito-nuclear



discordance, and male-biased dispersal of a large endangered snake, Drymarchon couperi. PLoS ONE. 14(3): e0214439.https://doi.org/10.1371/journal.pone.0214439.

Haacke WD. 1972. Herpetological field work in South-west Africa. Transvaal Mus. Bull. 12: 10-12. Hipondoka MH. 2005. The Development and Evolution of Etosha Pan, Namibia. Unpublished PhD dissertation, Julius-Maximilians-Universität Würzburg, Germany.

Hoetzel S, Dupont LM, Wefer G. 2015. Miocene-Pliocene vegetation change in south-western Africa (OPD Site 1081, offshore Namibia). Palaeogeogr Palaeoclimatol. Palaeoecol. 423:102–108. https:// doi.org/10.1016/j.palaeo.2015.02.002.

Jakobsson M, Rosenberg NA. 2007. CLUMPP: a cluster matching and permutation program for dealing with label switching and multimodality in analysis of population structure. Bioinformatics. 23(14): 1801–1806. https://doi.org/10.1093/bioinformatics/btm233.

Karin BR, Metallinou M, Weinell JL, Jackman TR, Bauer AM. 2016. Resolving the higher-order phylogenetic relationships of the circumtropical Mabuya group (Squamata: Scincidae): An outof-Asia diversification. Mol. Phylogenet. Evol. 102: 220-232. https://doi.org/10.1016/j.ympev. 2016.05.033.

Lanfear R, Frandsen PB, Wright AM, Senfeld T, Calcott B. 2017. PartitionFinder 2: New methods for selecting partitioned models of evolution for molecular and morphological phylogenetic analyses. Mol. Biol. Evol. 34(3): 772–773.

Laurent RF. 1964. Reptiles et amphbiens de l'Angola (Troisème contribution). Publicacões Culturais. Companhia de Diamantes de Angola. 67: 1–165.

Leigh JW, Bryant D. 2015. POPART: full-feature software for haplotype network construction. Methods Ecol. Evol. 6(9): 1110–1116. https://doi.org/10.1111/2041-210X.12410.

Macey JR, Larson A, Ananjeva NB, Papenfuss TJ. 1997. Evolutionary shifts in three major structural features of the mitochondrial genome among iguanian lizards. J. Mol. Evol. 44: 660-674. https://doi.org/10.1007/PL00006190.

Marques MP, Ceriaco LMP, Blackburn DC, Bauer AM. 2018. Diversity and distribution of the amphibians and terrestrial reptiles of Angola: Atlas of historical and bibliographic records (1840–2017). Proc. Calif. Acad. Sci. Series 4, 65, supplement II: 1–501.

Marques MP, Ceríaco LMP, Bandeira S, Pauwels OSG, Bauer AMB. 2019. Description of a new longtailed skink (Scincidae: Trachylepis) from Angola and the Democratic Republic of the Congo. Zootaxa. 4568(1): 51–68. https://doi.org/10.11646/zootaxa.4568.1.3.

Marshall TL, Chambers EA, Matz MV, Hillis DM. 2021. How mitonuclear discordance and geographic variation have confounded species boundaries in a widely studied snake. Mol. Phylogenet. Evol. 162: 107194.https://doi.org/10.1016/j.ympev.2021.107194.

Mausfeld P, Schmitz A, Böhme W, Misof B, Vrcibradic D, Rocha C. 2002. Phylogenetic affinities of Mabuya atlantica Schmidt, 1945, endemic to the Atlantic Ocean archipelago of Fernando de Noronha (Brazil): Necessity of partitioning the genus Mabuya Fitzinger, 1826 (Scincidae: Lygosominae). Zool. Anz. 241: 281-293. https://doi.org/10.1078/0044-5231-00081.

Mertens R. 1955. Die amphibien und reptilien Südwestafrikas, aus den ergebnissen einer im yahre 1952 ausgeführten reise. Abh. Senckenb. Naturforsch Ges. 490:1–172.

Mertens R. 1971. Die Herpetofauna Südwest-Afrikas. Abh. Senckenb. Naturforsch Ges. 529: 1–110. Metallinou M, Weinell JL, Karin BR, Conradie W, Wagner P, Schmitz A, Jackman TR, Bauer AM. 2016. A single origin of extreme matrotrophy in African mabuyine skinks. Biol. Lett. 12(8): 20160430. https://doi.org/10.1098/rsbl.2016.0430.

Miller MA, Pfeiffer W, Schwartz T. 2010. Creating the CIPRES Science Gateway for inference of large phylogenetic trees. 2010 Gateway Computing Environments Workshop (GCE), New Orleans, LA, USA, pp 1-8. https://doi.org/10.1109/GCE.2010.5676129.

Monard A. 1937. Contribution à l'herpétologie d'Angola. Arquivos do Museu Bocage. 8: 19-154.

Palumbi SR, Martin A, Romano S, McMillan WS, Stice S, Grabowski G. 1991. The Simple Fool's Guide to PCR. Honolulu: University of Hawaii Press.

Partridge TC, Maud RR. 1987. Ceomorphic evolution of southern Africa since the Mesozoic. S. Afr. J. Geol. 90(2): 179–208.

Portik DM. 2009. Comparative phylogeography of two skink species in Southern Africa. [MSc thesis]. Pennsylvania: Villanova University.



- Portik DM, Bauer AM, Jackman TR. 2010 The phylogenetic affinities of Trachylepis sulcata nigra and the intraspecific evolution of coastal melanism in the western rock skink. Afr. Zool. 45(2): 147–159. https://doi.org/10.3377/004.045.0217.
- Portik DM, Bauer AM, Jackman TR. 2011. Bridging the gap: Western rock skinks (Trachylepis sulcata) have a short history in South Africa. Mol. Ecol. 20(8): 1744-1758. https://doi.org/10.1111/j.1365-294X.2011.05047.x.
- Portik DM, Bauer AM. 2012. Untangling the complex: molecular patterns in Trachylepis variegata and T. punctulata (Reptilia: Scincidae). Afr. J. Herpetol. 61(2): 128-142. https://doi.org/10.1080/ 21564574.2012.721808.
- Pritchard JK, Stephens M, Donnelly P. 2000. Inference of population structure using multilocus genotype data. Genetics. 155(2): 945–959. https://doi.org/10.1093/genetics/155.2.945.
- Ronquist F, Teslenko M, van der Mark P, Ayres DL, Darling A, Höhna S, Larget B, Liu L, Suchard MA, Huelsenbeck JP. 2012. MrBayes 3.2: efficient Bayesian phylogenetic inference and model choice across a large model space. Syst. Biol. 61(3): 539-542. https://doi.org/10.1093/sysbio/sys029.
- Rosenberg NA. 2004. DISTRUCT: a program for the graphical display of population structure. Mol. Ecol. Notes. 4: 137-138. https://doi.org/10.1046/j.1471-8286.2003.00566.x.
- Sindaco R, Metallinou M, Pupin F, Fasola M, Carranza S. 2012. Forgotten in the ocean: systematics, biogeography and evolution of the Trachylepis skinks of the Socotra Archipelago. Zool. Scr. 41(4): 346-362. https://doi.org/10.1111/j.1463-6409.2012.00540.x.
- Stamatakis A. 2014. RAxML version 8: a tool for phylogenetic analysis and post- analysis of large phylogenies. Bioinformatics. 30(9): 1312-1313. https://doi.org/10.1093/bioinformatics/btu033.
- Stephens M, Donnelly P. 2003. A comparison of Bayesian methods for haplotype reconstruction from population genotype data. Am. J. Hum. Genet. 73(5): 1162-1169. https://doi.org/10.1086/ 379378.
- Stephens M, Smith NJ, Donnelly P. 2001. A new statistical method for haplotype reconstruction from population data. Am. J. Hum. Gen. 68: 978–989. https://doi.org/10.1086/319501.
- Toews DPL, Brelsford A. 2012. The biogeography of mitochondrial and nuclear discordance in animals. Mol. Ecol. 21: 3907–3930. https://doi.org/10.1111/j.1365-294X.2012.05664.x.
- Uetz P, Freed P, Aguilar R, Reyes F, Hošek J. 2023. The Reptile Database [accessed 4 December 2023]. http://www.reptile-database.org.
- Weinell JL, Bauer AM. 2018. Systematics and phylogeography of the widely distributed African skink Trachylepis varia species complex. Mol. Phylogenet. Evol. 120: 103–117. https://doi.org/10.1016/j. ympev.2017.11.014.
- Weinell JL, Branch WR, Colston TJ, Jackman TR, Kuhn A, Conradie W, Bauer AM. 2019. A species-level phylogeny of Trachylepis (Scincidae: Mabuyinae) provides insight into their reproductive mode evolution. Mol. Phylogen. Evol. 136: 183-195. https://doi.org/10.1016/j.ympev.2019.04.002.
- Werner F. 1915. Reptilia und Amphibia. In: Michaelsen W (ed.), Beiträge zur Kenntnis der Land- und Süsswasserfauna Deutsch-Südwestafrikas III. Hamburg: L. Friedrichsen & Co. pp. 325–376.
- Wielstra B, Arntzen JW. 2020. Extensive cytonuclear discordance in a crested newt from the Balkan Peninsula glacial refugium. Biol. J. Linn. Soc. Lond. 130: 578-585. https://doi.org/10.1093/ biolinnean/blaa062.
- Zheng Y, Wiens JJ. 2016. Combining phylogenomic and supermatrix approaches, and a time-calibrated phylogeny for squamate reptiles (lizards and snakes) based on 52 genes and 4162 species. Mol. Phylogen. Evol. 94: 537-547. https://doi.org/10.1016/j.ympev.2015.10.009.

Appendix Table A1: Museum accession numbers, locality information, and GenBank accession numbers for the samples used in this study. Sequences generated for this study are highlighted in bold.

AMB 9185 MUHNAC/MB03 1363 AMB 9658 MUHNAC/MB03 1343 AMB 9253 MUHNAC/MB03 1344 AMB 926 MUHNAC/MB03 1340 AMB 10926 INBAC AMB 10926 MUHNAC/MB03 1392 AMB 10909 MUHNAC/MB03 1394 AMB 10910 MUHNAC/MB03 1395 AMB 10911 MUHNAC/MB03 1391 AMB 10973 MUHNAC/MB03 1391 AMB 10873 CAS 263428 AMB 10823 CAS 263426	1363 Angola 1344 Angola 1340 Angola Angola Angola 1392 Angola 1395 Angola 1395 Angola 1391 Angola Angola Angola Angola Angola Angola Angola	Malanje Malanje Malanje Malanje Huambo Huambo Huambo Huambo Hufla Hufla Hufla	-9.748 -9.748 -9.748 -9.748 -12.424 -12.429 -12.429	15.132 15.132 15.132	OR183520 OR183523	OR188024 OR188027	OR214771 OR214773	OR214864 OR214865	OR214823 OR214825
		Malanje Malanje Malanje Huambo Huambo Huambo Huambo Hufla Hufla Hufla	-9.748 -9.748 -9.748 -12.424 -12.424 -12.429	15.132	OR183523	OR188027	OR214773	OR214865	OR214825
		Malanje Malanje Huambo Huambo Huambo Huambo Huambo Huila Huila Huila	-9.748 -9.748 -12.424 -12.429 -12.429	15.132			0117		4004
		Malanje Huambo Huambo Huambo Huambo Huambo Benguela Hufla Hufla	-9.748 -12.424 -12.424 -12.429	15 12 2	OK 183522	OR188026	OR214772		OK214824
		Huambo Huambo Huambo Huambo Huambo Benguela Huíla Huíla	-12.424 -12.424 -12.429 -12.429	201.01	OR183521	OR188025			
		Huambo Huambo Huambo Huambo Benguela Huíla Huíla	-12.424 -12.429 -12.429	15.149	OR183543	OR188047	OR214790	OR214874	OR214837
		Huambo Huambo Huambo Huambo Benguela Huíla Huíla	-12.429 -12.429	15.149	OR183544	OR188048	OR214791		
		Huambo Huambo Huambo Benguela Huíla Huíla	-12.429	15.154	OR183539	OR188043	OR214788	OR214872	OR214835
		Huambo Huambo Benguela Hufla Hufla Namibe		15.154	OR183540	OR188044	OR214789	OR214873	OR214836
		Huambo Benguela Huíla Huíla Namibe	-12.429	15.154	OR183541	OR188045			
		Benguela Huíla Huíla Namibe	-12.429	15.154	OR183542	OR188046			
	Angola Angola Angola Angola Angola	Huíla Huíla Huíla Namibe	-13.044	14.053	OR183545	OR188049	OR214792	OR214875	OR214838
	Angola Angola Angola Angola	Huíla Huíla Namibe	-13.755	15.042	OR183537	OR188041	OR214786	OR214870	OR214833
	Angola Angola Angola	Huíla Namibe	-13.755	15.042	OR183538	OR188042	OR214787	OR214871	OR214834
	Angola Angola	Namibe	-13.755	15.042	OR183536	OR188040			
_	Angola		-13.777	13.259	OR183524	OR188028	OR214774		
_		Namibe	-13.777	13.259	OR183525	OR188029	OR214775		
_	Angola	Namibe	-13.777	13.259	OR183526	OR188030	OR214776		
	Angola	Namibe	-13.781	13.258	OR183528	OR188032	OR214778		OR214827
	Angola	Namibe	-13.786	13.257	OR183529	OR188033	OR214779		OR214828
_	Angola	Namibe	-13.786	13.257	OR183527	OR188031	OR214777	OR214866	OR214826
_	Angola	Namibe	-13.807	13.135	OR183535	OR188039	OR214785	OR214869	OR214832
_	Angola	Namibe	-13.810	13.136	OR183533	OR188037	OR214783	OR214868	OR214831
•	Angola	Namibe	-13.810	13.136	OR183534	OR188038	OR214784		
	Angola	Namibe	-13.811	13.136	OR183530	OR188034	OR214780	OR214867	OR214829
_	Angola	Namibe	-13.811	13.136	OR183531	OR188035	OR214781		OR214830
Ŭ	Angola	Namibe	-13.811	13.136	OR183532	OR188036	OR214782		
ET 35, ARG 199 F	Angola	Huíla	-13.972	14.047	OR183548		OR214793		
	Angola	Huíla	-14.824	13.381	OR183554	OR188055	OR214799	OR214881	OR214844
	Angola	Huíla	-14.824	13.381	OR183559	OR188060	OR214804	OR214885	OR214848
	Angola	Huíla	-14.824	13.381	OR183561	OR188062	OR214805	OR214886	OR214849
AMB 10146 CAS 263343	Angola	Huíla	-14.824	13.381	OR183555	OR188056	OR214800		
AMB 10693 CAS 263345	Angola	Huíla	-14.824	13.381	OR183560	OR188061			
AMB 11169 MHNC-UP/REP 460	60 Angola	Huíla	-14.844	15.036	OR183546	OR188066	OR214809	OR214888	OR214851
AMB 11170 MHNC-UP/REP 461	61 Angola	Huíla	-14.844	15.036	OR183547				

(Continued)

(Continued)

Collector No.(s)	Accession No.	Country	Province/Region	Latitude	Longitude	16s	ND2	Rag1	MXRA5	EXPH5
AMB 10838	CAS 263333	Angola	Huíla	-14.940	13.512	OR183562	OR188063	OR214806	OR214887	OR214850
AMB 10842	CAS 263336	Angola	Huíla	-14.940	13.512	OR183563	OR188064	OR214807		
AMB 10844	CAS 263338	Angola	Huíla	-14.940	13.512	OR183564	OR188065	OR214808		
AMB 8573	CAS 254886	Angola	Namibe	-15.045	13.159	OR183566	OR188068	OR214811	OR214890	OR214853
AMB 8565	CAS 254888	Angola	Namibe	-15.045	13.159	OR183567	OR188069			
AMB 8544	CAS 254875	Angola	Namibe	-15.070	13.243	OR183565	OR188067	OR214810	OR214889	OR214852
AMB 10503	CAS 263516	Angola	Namibe	-15.871	12.903	OR183550	OR188051	OR214795	OR214877	OR214840
AMB 10504	INBAC	Angola	Namibe	-15.938	12.884	OR183551	OR188052	OR214796	OR214878	OR214841
AMB 10388	CAS 263520	Angola	Namibe	-15.950	12.495	OR183549	OR188050	OR214794	OR214876	OR214839
AMB 10639	CAS 263489	Angola	Namibe	-16.295	12.941	OR183556	OR188057	OR214801	OR214882	OR214845
AMB 10640	CAS 263490	Angola	Namibe	-16.295	12.941	OR183557	OR188058	OR214802	OR214883	OR214846
AMB 10641	CAS 263491	Angola	Namibe	-16.295	12.941	OR183558	OR188059	OR214803	OR214884	OR214847
AMB 10542	CAS 263484	Angola	Namibe	-16.310	12.796	OR183552	OR188053	OR214797	OR214879	OR214842
AMB 10543	CAS 263485	Angola	Namibe	-16.310	12.796	OR183553	OR188054	OR214798	OR214880	OR214843
MCZ A38932	MCZ R185901	Namibia	Kunene	-19.649	14.359	OR183575	GU931594	GU931662	OR214893	GU931422
MCZ A27704	MCZ R190247	Namibia	Kunene	-17.000	13.233	0R183576	OR188072	OR214815	0R214894	OR214856
MCZ 38958	MCZ R185905	Namibia	Kunene	-17.290	13.159		GU931595	GU931663		GU931416
AMB 8033	MCZ R190197	Namibia	Omusati	-17.414	14.355	OR183572	OR188070	OR214812	OR214891	OR214854
AMB 8043	MCZ R190207	Namibia	Kunene	-17.434	13.994	OR183573	OR188071			OR214855
AMB 6971	SMW	Namibia	Kunene	-18.213	13.800	OR183568	GU931559	GU931627		GU931417
AMB 6981	CAS 223996	Namibia	Kunene	-18.213	13.800	OR183571	GU931560	GU931628		GU931419
Mab 129,	CAS 223979	Namibia	Kunene	-18.213	13.800	MK792054	GU931561	GU931629		GU931418
AMB 6987										
AMB 6972	SMW	Namibia	Kunene	-18.213	13.800	OR183569		HQ829776		
AMB 6979	CAS 223994	Namibia	Kunene	-18.213	13.800	OR183570		HQ829777		
ZFMK 66424	ZFMK 66424	Namibia	Kunene	-19.140	13.819	OR183519				
MCZ 38521	MCZ R184875	Namibia	Otjozondjupa	-19.552	17.236	OR183515	GU931589	GU931657		GU931420
E 111037	Enviro-Insight	Namibia	Kunene	-19.625	14.842	OR183486				
Mab 162,	SMW	Namibia	Kunene	-19.630	14.816	OR183510	GU931584	GU931652		GU931421
MCZ Z37867										
Mab 127, AMB 6895	SMW	Namibia	Kunene	-19.683	14.319	OR183500	GU931558	GU931626		GU931423
MCZ 23125	MCZ R185913	Namibia	Kunene	-19.859	15.196	OR183574	GU931581	GU931649	OR214892	GU931424
MCZ A28758	MCZ R193220	Namibia	Kunene	-20.422	15.461	OR183580	OR188076	OR214819	OR214897	OR214860
MCZ A28324	MCZ R193126	Namibia	Erongo	-21.498	15.630	OR183579	OR188075	OR214818		OR214859
MCZ A28823	MCZ R193268	Namibia	Otjozondjupa	-21.977	16.934	OR183581	OR188077	OR214820	OR214898	OR214861
MCZ A28846		Namibia	Khomas	-22.805	16.965	OR183582	OR188078	OR214821	OR214899	OR214862
MCZ A28068	MCZ R190339	Namibia	Hardap	-23.626	16.693	OR183577	OR188073	OR214816	OR214895	OR214857

Continued.		,		-		,				11.00
	Accession No.	Country	Province/Region	Latitude	Longitude	16s	ND2	Rag1	MXRA5	EXPH5
	MCZ R193115	Namibia	Hardap	-24.152	16.014	OR183578	OR188074	OR214817	OR214896	OR214858
	MCZ R193302	Namibia	Hardap	-24.498	17.870	OR183583	OR188079	OR214822	OR214900	OR214863
	MCZ R184343	Namibia	Hardap	-25.415	16.797	OR183509	GU931585	GU931653		GU931425
	MCZ R185917	Namibia	Karas	-25.897	17.777		GU931582	GU931650		GU931426
	MCZ R185918	Namibia	Karas	-25.897	17.777		GU931583	GU931651		GU931427
	MCZ R185047	Namibia	Karas	-26.147	16.569		GU931590	GU931658		GU931428
	MCZ R185064	Namibia	Karas	-26.605	18.478		GU931592	GU931660		GU931429
	MCZ R185923	Namibia	Karas	-26.614	15.171	OR183517		GU931664		GU931460
	MCZ R185924	Namibia	Karas	-26.614	15.171	OR183518	OR188080	GU931665		GU931461
	SMW	Namibia	Karas	-26.619	18.124	OR183487	GU931562	GU931630		GU931430
	MCZ R185006	Namibia	Karas	-26.677	16.228	OR183516	GU931591	GU931659		GU931431
	MCZ R184351	Namibia	Karas	-26.749	17.221	OR183503	GU931586	GU931654		GU931432
	SMW	Namibia	Karas	-26.749	17.221	OR183502		HQ829801		
MCZ A38293										
	MCZ R184386	Namibia	Karas	-27.376	18.493	OR183504		OR214813		
	SMW	Namibia	Karas	-27.376	18.495	OR183506	GU931587	GU931655		GU931433
	MCZ R184820	Namibia	Karas	-27.376	18.493	OR183513				
	MCZ R184821	Namibia	Karas	-27.376	18.493	OR183514				
	MCZ R184374	Namibia	Karas	-27.382	18.477	OR183505		HQ829803		
MCZ A38357										
	MCZ R184375	Namibia	Karas	-27.382	18.477	OR183508		OR214814		
	SMW	Namibia	Karas	-27.386	18.492	OR183507				
	MCZ R185113	Namibia	Karas	-27.494	19.222		GU931593	GU931661		GU931434
	CAS 223993	Namibia	Karas	-27.882	18.789	OR183501	GU931557	GU931625		GU931435
	SMW	Namibia	Karas	-27.882	18.789	OR183499		HQ829774		
	PEM R17732 LSUMZ 57296	Namibia South Africa	Karas Northern Cape	-27.914 -28.163	17.491 17.019	OR183493	GU931564	GU931632		GU931436
	PEM R11868	South Africa	Northern Cape	-28.203	17.110	OR183494	GU931554	GU931622		GU931437

	•
(44	Ŀ
\sim	

Collector No.(s)	Accession No.	Country	Province/Region	Latitude	Longitude	16s	ND2	Rag1	MXRA5	EXPH5
Mab 103,	CAS 200043	South Africa	Northern Cape	-28.334	16.907	OR183491	GU931552	GU931620		GU931439
AMB 4590 Mab 106,	PEM R11875	South Africa	Northern Cape	-28.342	16.977	OR183492	GU931553	GU931621		GU931440
AINIB 4620 JM 1186	PEM R17733	South Africa	Northern Cape	-28.373	16.828		GU931566	GU931634		GU931441
Mab 114,	LSUMZ 57297	South Africa	Northern Cape	-28.425	17.001	OR183496	GU931556	GU931624		GU931442
AMB 4782										
MB 20804	PEM R17104	South Africa	Northern Cape	-28.625	21.753		GU931574	GU931642		GU931443
MB 20892	PEM or NMB	South Africa	Northern Cape	-29.049	22.260		GU931575	GU931643		GU931444
MCZ 38432	MCZ R184770	South Africa	Northern Cape	-29.316	17.087	OR183512	GU931588	GU931656		GU931445
Mab 100,	PEM R11914	South Africa	Northern Cape	-29.338	17.792	OR183490				
AMB 4291										
MB 21191	PEM R19070	South Africa	Northern Cape	-30.144	23.471		GU931577	GU931645		GU931446
JM 1119	PEM R17744	South Africa	Northern Cape	-30.352	17.885		GU931565	GU931633		GU931447
MBUR 01798	PEM	South Africa	Northern Cape	-30.410	18.096		GU931580	GU931648		GU931448
MBUR 01797	PEM	South Africa	Northern Cape	-30.410	18.096	OR183511		HQ829800		
MB 20644	PEM R17050	South Africa	Northern Cape	-30.578	19.342		GU931570	GU931639		GU931450
MB 20689	PEM R17058	South Africa	Northern Cape	-30.591	18.822		GU931572	GU931640		GU931449
Mab 99	CAS 199999	South Africa	Northern Cape	-30.613	18.021	OR183489				
MB 20720	PEM R17052	South Africa	Northern Cape	-30.925	19.048		GU931573	GU931641		GU931451
MB 21140	NMB R9254	South Africa	Northern Cape	-30.931	23.232		GU931576	GU931644		GU931452
MB 20632	PEM R17098	South Africa	Northern Cape	-31.194	19.305		GU931571	GU931638		GU931453
AMB 8171	MCZ R184394	South Africa	Eastern Cape	-32.101	26.255		GU931563	GU931631		GU931454
Mab 51,	MCZ R184395	South Africa	Eastern Cape	-32.101	26.255	OR183488		HQ829778		
AMB 8172										
KTH 200	PEM	South Africa	Western Cape	-32.281	20.106		GU931567	GU931635		GU931455
MBUR 00603	PEM R17045	South Africa	Eastern Cape	-32.874	24.489		GU931578	GU931646		GU931456
MBUR 00726	PEM	South Africa	Western Cape	-33.123	22.333		GU931579	GU931647		GU931457
Mab 121	CAS 180413	South Africa	Western Cape	-33.736	21.606	OR183498	GU931569	GU931637		GU931458
KTH 538	SAM	South Africa	Western Cape	-33.952	20.458		GU931568	GU931636		GU931459
Mab 113,	PEM R12413	South Africa	Northern Cape			OR183495	GU931555	GU931623		GU931438
AMB 4/6/ Mab 115,	LSUMZ 57298	South Africa	Northern Cape			OR183497				
AMB 4790			-							

Continued.